Molecular Medicine

Antiangiogenic and Antitumoral Effects Mediated by a Vascular Endothelial Growth Factor Receptor 1 (VEGFR-1)-Targeted DNAzyme

Liangfang Shen,[1] Qin Zhou,[1] Ying Wang,[1] Weihua Liao,[2] Yan Chen,[4] Zhijie Xu,[3] Lifang Yang,[3,4] and Lun-Quan Sun[4]

Departments of [1]Oncology and [2]Radiology, Xiangya Hospital, Central South University, Changsha, Hunan, China; [3]Cancer Research Institute, Central South University, Hunan, China; and [4]Center for Molecular Medicine, Xiangya Hospital, Central South University, Changsha, Hunan, China

Antiangiogenesis is a promising antitumor strategy that inhibits tumor vascular formation to suppress tumor growth. DNAzymes are synthetic single-strand deoxyribonucleic acid (DNA) molecules that can cleave ribonucleic acids (RNAs). Here, we conducted a comprehensive *in vitro* selection of active DNAzymes for their activity to cleave the vascular endothelial growth factor receptor (*VEGFR-1*) mRNA and screened for their biological activity in a matrigel tube-formation assay. Among the selected DNAzymes, DT18 was defined as a lead molecule that was further investigated in several model systems. In a rat corneal vascularization model, DT18 demonstrated significant and specific antiangiogenic activity, as evidenced by the reduced area and vessel number in VEGF-induced corneal angiogenesis. In a mouse melanoma model, DT18 was shown to inhibit B16 tumor growth, whereas it did not affect B16 cell proliferation. We further assessed the DT18 effect in mice with established human nasopharyngeal carcinoma (NPC). A significant inhibition of tumor growth was observed, which accompanied downregulation of VEGFR-1 expression in NPC tumor tissues. To evaluate DT18 effect on vasculature, we performed dynamic contrast enhanced magnetic resonance imaging (DCE-MRI) on the human NPC xenograft mice treated with DT18 and showed a reduction of the parameter of K^{trans} (volume constant for transfer of contrast agent), which reflects the condition of tumor microvascular permeability. When examining the safety and tolerability of DT18, intravenous administration of Dz18 to healthy mice caused no substantial toxicities, as shown by parameters such as body weight, liver/kidney function, and histological and biochemical analyses. Taken together, our data suggest that the anti-*VEGFR-1* DNAzyme may be used as a therapeutic agent for the treatment of cancer, such as NPC.

Online address: http://www.molmed.org
doi: 10.2119/molmed.2013.00090

INTRODUCTION

Angiogenesis is a physiological process required for embryonic development, the menstrual cycle and wound healing (1,2). A large number of human diseases are also characterized by abnormal angiogenesis, such as tumor growth and metastasis (3). An abnormal vasculature is a hallmark of solid tumors. The angiogenic process involves interaction between angiogenic factors and endothelial cells (ECs) and can be manipulated directly or indirectly. Thus, depriving the tumor of the excessive vessels that support its growth became the target for developing antiangiogenic agents that could provide, in combination with chemo- or radiotherapy, improved anticancer treatment (4).

In contrast to conventional cytotoxic agents, antiangiogenic agents work by blocking oxygen and nutrient supplies to tumors, thereby suppressing their growth. This approach has several theoretical advantages. First, ECs are a genetically stable, diploid and homogenous target, and spontaneous mutations rarely occur. An antiangiogenic agent is less likely than a cytotoxic agent to induce drug resistance because it targets genetically stable ECs instead of genetically unstable tumor cells (5). Second, an antiangiogenic approach would have fewer off-target side effects because only tumor-associated ECs proliferate and express specific markers, such as integrin αvβ3, E-selectin and vascular endothelial growth factor (VEGF) receptors, unlike quiescent normal ECs (5). Finally, different tumor cells are sus-

Address correspondence to *Lun-Quan Sun, 87 Xiangya Road, Changsha, Hunan, China, 410078. Phone: +86-731-84327646; Fax: +86-731-84327212; E-mail: lunquansun@csu.edu.cn; or Lifang Yang, 110 Xiangya Road, Changsha, Hunan, China, 410078. Phone: +86-731-84805448; Fax: +86-731-84470589; E-mail: yanglifang@csu.edu.cn.*
Submitted August 14, 2013; Accepted for publication October 29, 2013; Epub (www.molmed.org) ahead of print October 30, 2013.

The Feinstein Institute for Medical Research North Shore LIJ

tained by a single capillary, and tumor-associated ECs contribute both to endothelial and tumor cell growth by releasing autocrine and paracrine factors. Consequently, the activated endothelium presents a more specific target than the tumor cells, and inhibition of a small number of tumor vessels may affect the growth of many tumor cells.

The two major tyrosine kinase receptors for VEGFA are VEGFR-1 and VEGFR-2. Unlike fibroblast growth factor receptors, both VEGF receptors are selectively expressed on ECs (6). Expression of *VEGFR-1* messenger ribonucleic acid (mRNA) is hypoxia-inducible, and EC expression of VEGFR-2 is induced in ischemic tissue via a paracrine mechanism (7,8). Depending on the tumor type, VEGF and its two receptors may function via either of the autocrine or paracrine mechanisms in humans (9). In comparison to the surrounding normal tissue vasculature, both VEGFR-1 and VEGFR-2 are upregulated in tumor-associated ECs in a variety of tumors (10). The primary role of VEGFR-1 is to regulate the assembly of ECs into tubes, whereas VEGFR-2 induces permeability and EC differentiation and proliferation (11). Because the elevated expression of VEGF and its receptors is closely correlated with tumor vascularity, progression and metastasis (12,13), targeting *VEGF*/*VEGFRs* becomes quite a worthwhile strategy. Several strategies have been developed to inhibit VEGF activity, including inhibition of VEGF induction, neutralization of free unbound VEGF, blockade of VEGFR activity and inhibition of downstream intracellular signaling (14).

The 10-23 deoxyribonucleic acid (DNA) enzyme or DNAzyme was named from its origin as the 23rd clone characterized from the 10th cycle of *in vitro* selection (15). This enzyme has a number of features that give it tremendous potential for applications both *in vitro* and *in vivo*. These features include its ability to cleave almost any RNA sequence with high specificity, provided that the sequence contains a purine-pyrimidine dinucleotide. This step can be accomplished at very high kinetic efficiency, with rates approaching and even exceeding those of other nucleic acid and protein endoribonucleases (16). The ability of the 10-23 DNAzyme to specifically cleave RNA with high efficiency under simulated physiological conditions has fuelled expectation that this agent may have useful biological application in a gene inactivation strategy (17,18). Accumulating evidence indicates the utility, efficacy and potency of DNAzymes in a variety of animal models of disease and human cancers, allowing characterization of key molecular pathways underlying pathogenesis and use as a therapeutic agent (19–23).

In the present study, we conducted a comprehensive screening of the *VEGFR-1*-targted DNAzymes both *in vitro* and in cells. The lead molecule DT18 was assessed in several relevant *in vivo* models and generated significant data of clinical relevance to cancer therapy.

Materials and Methods

Cell Cultures

Human umbilical vein endothelial cells (HUVECs) were purchased from ScienCell (Carlsbad, CA, USA) and cultured in endothelial cell medium. B16 cells (ATCC CRL-6322; American Type Culture Collection (ATCC), Manassas, VA, USA) and CNE1-LMP1 (24) cells were maintained according to vendor recommendations.

DNAzyme Synthesis

All the oligonucleotides were made by Oligos Etc. Inc. (Wilsonville, OR, USA) and were purified by gel electrophoresis for *in vitro* studies and by high-performance liquid chromatography for cell-based assays and *in vivo* studies.

Design and Thermodynamic Analysis of DNAzymes

DNAzyme sequences for each target are assembled using the 10-23 catalytic motif (GGCTAGCTACAACGA) and hybridizing arms specific for each site along the target RNA transcript. The length of each arm is usually fixed at six to nine bases, depending on their individual predicted hybridization-free energy (25). Each DNAzyme oligonucleotide is designed to target purine-uracil (RU; R = G or A). In most cases, we ignore purine-cytosine sites, since in our experience, they are less reactive than RU sites (particularly AC junctions) (26). The potential DNAzymes and INV-Ctrl (a control molecule with an inverted catalytic core) were subjected to thermodynamic analyses (19).

In Vitro Cleavage and Kinetic Assay of DNAzymes

To prepare the substrates used in the mRNA cleavage experiment, *in vitro* transcription using T7 RNA polymerase was carried out. A transcription template was a plasmid encoding the soluble fraction of the *VEGFR-1* gene driven by a T7 promoter. The template was transcribed in a 10-μL volume of reaction at 37°C for 2 h in the presence of [γ-^{32}P]UTP with a T7 Ampliscribe transcription kit (Epicentre, Madison, WI, USA).

To determine the RNA cleavage activity of each DNAzyme, they were combined with the RNA transcript and placed at 85°C for 30 s, followed by incubation at 37°C for 5 min and further incubated for 60 min in 50 mmol/L Tris-Cl and 10 mmol/L $MgCl_2$, pH 7.5. Reactions were terminated by adding to equal volumes of stop buffer (98% formamide, 10 mmol/L EDTA and 0.1% loading dye). To analyze the cleavage reactions, the samples were run on a 6% denaturing polyacrylamide gel at 75 W for 1 h. The gel was then exposed on a PhosphorImager, and the bands were quantified by using the ImageQuant software TL (GE Healthcare, Milwaukee, WI, USA).

For kinetic analyses, a ^{32}P-labeled RNA oligonucleotide corresponding to each DNAzyme was incubated with a 10-fold excess of DNAzyme oligonucleotide at 37°C for t = 0, 5, 10, 20, 30 and 60 min. The reaction conditions, electrophoresis and analysis of the cleav-

age reactions were otherwise the same as that described above. The percentage of band intensity in the cleavage products was then analyzed graphically in a plot against time. A curve was generated for the data (least-squares) by using the equation $\%P = \%P_\infty - C \cdot \exp[-kt]$, where $\%P$ is the percentage product, $\%P_\infty$ is the percentage product at $t = \infty$, C is the difference in $\%P$ between $t = \infty$ and $t = 0$, and k is the first order rate constant (27). The first order rate constant (k_{obs}) was used to determine the cleavage efficiency.

DNAzyme Transfection of HUVECs

To assay the DNAzymes' activity in HUVECs, transfection conditions were optimized with a cationic porphyrin reagent known as meso-tetra (4-methylpyridyl) porphine porphyrin (TMP) (28). Approximately 6×10^5 HUVECs were seeded in each 60-mm dish 1 d before transfection. Cells reached approximately 80–90% confluency after being incubated at 37°C overnight. TMP-DNAzyme complexes were formed 15 min before introducing to the cells, with the charge ratio (TMP:DNAzyme) of 3. Cells were washed with serum-free medium and then treated with the complex overnight (final DNAzyme concentration of 1 μmol/L). At 24-h posttransfection, cells were allowed to recover in complete medium overnight. Cells were harvested the next day by trypsinization to detach the cells and washed twice with phosphate-buffered saline. A 5′ fluorescein isothiocyanate (FITC)-labeled DNAzyme oligonucleotide was used for assessing transfection efficiency via fluorescence-activated cell sorter (FACS) analyses.

Western Analysis

Protein was extracted from the transfected cells in radioimmunoprecipitation assay buffer (50 mmol/L Tris-HCl, pH 8, 150 mmol/L NaCl, 0.1% sodium dodecyl sulfate, 1% NP-40, 0.5% sodium deoxycholate, 0.57 mmol/L phenylmethylsulfonyl fluoride and 1 μg/mL aprotinin). Protein samples (40 μg) were run on 12% sodium dodecyl sulfate–polyacrylamide gel electrophoresis gels (Bio-Rad), transferred to nylon membranes and immunoblotted with the anti-VEGFR-1 mouse monoclonal antibody (Santa Cruz Biotechnology, Santa Cruz, CA, USA) and anti-β-actin monoclonal antibody (AC-74; Sigma-Aldrich, St. Louis, MO, USA). Binding of primary antibodies was detected with goat anti-rabbit or anti-mouse horse radish peroxidase–conjugated secondary antibodies (Santa Cruz Biotechnology). This binding was visualized with the Amersham ECL Western blotting detection reagents (GE Healthcare, Milwaukee, WI, USA) on exposure to chemiluminescent film.

Tube Formation Assay

A Matrigel angiogenesis assay has been developed for testing the antiangiogenic activity of the DNAzymes on the basis of the differentiation of ECs on a basement membrane matrix (Matrigel; BD Biosciences, San Jose, CA, USA) derived from the Engelbreth-Holm-Swarm tumor. Briefly, HUVECs were seeded in each well of the six-well plate (~1.4×10^4 cells/well) 1 d before transfection. Cells reached approximately 80–90% confluency after being incubated at 37°C overnight. DNAzymes were delivered with the transfection reagent TMP. The complexes were formed 15 min before introducing to the cells as described. The final concentration of the DNAzymes was 1 μmol/L with the charge ratio of 3 (TMP:DNAzyme). Cells were washed with serum-free medium, treated with the complex for 3 h and then allowed to recover in complete medium overnight. Transfected cells were trypsinized and centrifuged at 600*g* for 6 min. The cell pellets were washed once in serum-supplemented media and centrifuged again as described above. Approximately 30,000 cells were seeded in each well of a 96-well plate with 100 μL Matrigel embedded. Medium was replaced with low serum medium after 2 h, and cells were cultured overnight. The following day, the extent of tube-forming activity was examined by low-magnification microscopy and documented by digital photomicrography.

Corneal Vascularization Assay

The cornea presents an *in vivo* avascular site. Therefore, any vessels penetrating from the limbus into the corneal stroma can be identified as newly formed. To induce an angiogenic response, nitrocellulose filter disks imbibed with VEGF are implanted in corneal stromal pockets of the rat (27). The vascular response occurs within days and can be quantified optically under a microscope or by computer image analysis. Briefly, all rats were maintained and manipulated according to strict guidelines set out by the Medical Research Animal Ethics Committee (Central South University, China). In the experiments, the corneas of 7-wk-old male Sprague Dawley rats were implanted with a 30 μmol/L VEGF-soaked nitrocellulose filter disk. Each disk was soaked with this solution in an Eppendorf tube on ice for 2 h before implantation. Depending on the group, saline (carrier), 100 μg *VEG*FR-1 DNAzyme, or its control oligonucleotide was administered to the conjunctiva adjacent to the implant site on the day of disk implantation. On d 5 after implantation, the corneas were removed to quantitate the area covered by vascularization. Vessel count was assessed by light microscopy in areas of the corneas implanted with the VEGF disk. After the area of highest neovascularization was identified, a vessel count was performed on a 200× field (20× objective and 10× ocular, 0.739 mm^2 per field).

Mouse Tumor Models

All mice were maintained and manipulated according to strict guidelines set out by the Medical Research Animal Ethics Committee (Central South University, China). For the murine B16 melanoma model, Matrigel (0.2 mL, 50%) containing 5×10^4 B16 (murine melanoma) cells + 100 μg DT18 (with 2.5 μL transfection reagent Fugene6 [Roche, Indianapolis, IN, USA]), its

control oligonucleotide or saline was injected subcutaneously into the shaved dorsal midback region of 5-wk-old C57BL/J6 female mice. Each group had at least eight mice per group. Mouse weights and tumor dimensions were recorded thrice weekly.

For the human nasopharyngeal carcinoma xenograft model, 6-wk-old female athymic nude mice were injected subcutaneously with 5×10^6 CNE1-LMP1 cells (five mice per group). Tumors were measured on alternate days by using a caliper, and tumor volumes were calculated using the following formula: (length × width × height) × (π/6). When the tumor volume reached 60–100 mm^3, the animals were injected intratumorally with 100 μg DT18 or INV-Ctrl with 3 μL Fugene6 or saline alone twice a week in an injectate volume of 20 μL. At the end of the experiments (d 18 from the first treatment), mice were killed humanely and tumor tissues were stored for histochemical examination.

Dynamic Contrast Enhanced Magnetic Resonance Imaging (DCE-MRI)

MRI was performed 3 d after the DT18 treatment. All data were acquired on superconducting magnetic resonance imaging scanners (Signa HDx 3.0T, GE Healthcare, Milwaukee, WI, USA) with a coil of 2.0 inches diameter for animal experiments (FT-AN; Fei-Te Technologies Inc, Shanghai, China). Mice were anesthetized by using 10% chloral hydrate. MRI regular scan: T2 weighted imaging (T2WI) coronary images use turbo spin echo (TSE) sequence, echo time (TE) = 105 ms, repetition time (TR) = 2,000 ms, field of view (FOV) = 80 mm over a 160 × 128 matrix, number of excitations (NEX) = 2, layer thickness = 2 mm, layer number = 8, interlayer spacing = 0.1. T2W1 section images use TSE sequence, TR = 2,100 ms, TE = 60 ms, FOV = 40 mm over a 160 × 128 matrix, NEX = 4, layer thickness = 2 mm, layer number = 10, interlayer spacing = 0.1; T1W1 section images use TSE sequence TR = 625 ms, TE = 15 ms; the rests are similar with T2W1 section images. DCE-MRI uses the 3DSPGR sequence, refers to the T2W1 images, TR = 16.3 ms, TE = 1.9 ms, flip angle 30°, FOV = 40 mm over a 108 × 128 matrix, actual layer thickness = 2.2 mm, layer number = 4, spatial resolution 0.31 × 0.37 × 2.2 mm^3, time resolution 18 s with 60 time phase, total imaging time 18 min 18 s. On the eighth time phase, Gd-DTPA, a blood-pool contrast agent, was injected via the tail-vein catheter (within 3 s). The raw data of DCE-MRI were analyzed using NordicICE software (version 2.3.6; NordicNeuroLab, Bergen, Norway) without knowing animal grouping information.

Immunohistochemistry

Tissue specimens were fixed with 10% neutral-buffered formalin, and 4-mm paraffin sections were then prepared. The sections were immunostained by using a streptavidin peroxidase procedure after microwave antigen retrieval. The primary antibody was anti-VEGF (1:50; Santa Cruz Biotechnology). Specimens were incubated with the biotinylated secondary antibody (BioGenex, Fremont, CA, USA) against the primary antibody and then with the avidin-biotin-peroxidase complex. Visualization was performed by using diaminobenzidine (DAB) (BioGenex). A negative control was run for each slide by using an irrelevant, isotype antibody. All immunostained sections were then lightly counterstained with Mayer hematoxylin.

Toxicological and Pharmacokinetic Study

Three groups of six Balb/C mice (6–8 wks old, even number of male and female) were injected with DT18 (20 mg/kg), INV-Ctrl (20 mg/kg) or saline via an intravenous route. Mice in each group were observed and weighed daily. Blood was collected via retro-orbital sinus puncture at various time points, and tissues from euthanized animals were collected. Specimens were processed for clinical pathology, including hematological and serum chemistry, immunological and histopathological evaluations. A histopathological assessment was made of sectioned and hematoxylin- and eosin-stained tissues by a board-certified veterinary pathologist.

To determine pharmacokinetics of DT18, ^{32}P end–labeled DT18 (200 μL at 1 mg/mL) was intravenously administrated into mice (10 mg/kg, three mice per group). The blood samples (0.5 mL) were taken at 2, 4, 8, 10, 15, 20 and 30 min and 1, 2, 4, 8, 24 and 48 h. Plasma was collected by centrifugation, and DT18 was extracted by phenol/chloroform. Samples were assayed by Southern blots and quantitated as a function of absolute concentration derived from a standard curve. Pharmacokinetic parameters were calculated by using PK Solution software (SummitPK, Montrose, CO, USA).

Statistical Analysis

Data are presented as mean ± SE and analyzed by one-way analysis of variance (ANOVA) followed by the Dunnett test. All analyses were performed by using SPSS for Windows 16.0. $P < 0.05$ was considered statistically significant.

RESULTS

Design of *VEGFR-1* DNAzymes Targeted to Conserved Regions among Mouse/Rat and Human *VEGFR-1* mRNA

For anti–*VEGFR-1* DNAzymes to be screened in human cells and tested in mouse models, it is necessary to make DNAzymes that would target both human and murine/rat sequences. Human and mouse/rat sequences of *VEGFR-1* mRNA were aligned to look for the consensus sequences. After a comprehensive analysis, 11 potential target sites were identified on the basis of the sequence homology. Constructed DNAzymes were composed of either symmetric or asymmetric arms because of the restriction from the length of the consensus sequence. Individual DNAzymes were assessed by using the nearest neighbor formula for the free energy of hybridization ($\Delta G°$) of each hybridizing arm. The arm length of each

Table 1. DNAzyme target site, arm length, sequences and activity in tube formation assays.

DNAzymes	Target sites	Arms	Sequence (5′ to 3′)[a]	Activity[b]
DT10	250	9/7	AGCTGACCAGGCTAGCTACAACGAGGTGAGC	+
DT11	353	9/7	CCTTTTAAAGGCTAGCTACAACGATCAGTTC	–
DT12	843	8/9	TCTTTGTAGGCTAGCTACAACGAGTTGCATTT	+
DT13	943	8/5	TATTTGGAGGCTAGCTACAACGAATCTA	–
DT14	1324	7/6	GCCTTCAGGCTAGCTACAACGATTTCAT	+
DT15	1592	7/7	TTGTCTGGGCTAGCTACAACGATGCCCAG	+
DT16	1753	9/9	TGCTCTCAAGGCTAGCTACAACGATCTGTTTCC	–
DT17	1910	6/6	GGCACAGGCTAGCTACAACGACTGTGA	+
DT18	2098	7/5	AGAGTGAGGCTAGCTACAACGAGGAGT	+ +
DT19	2161	7/6	TTCCTGGGGCTAGCTACAACGATCTGCA	+
DT20	2323	9/7	ACCAAGTGAGGCTAGCTACAACGACTGAGGC	–

[a]DNAzymes were constructed with either symmetric or asymmetric arms depending on the length of the consensus sequence and free energy; the catalytic core sequence was underlined.
[b]The activity was assessed based on no disruption (–), partial disruption (+) and complete disruption (++) of the tube structures in the Matrigel assay.

DNAzyme was slightly adjusted to ensure that each had the $\Delta G° \leq -10$ kcal/mol per arm (19). As a result, 11 DNAzymes targeted to the selected sites were synthesized for assessments (Table 1).

In Vitro Screening of Anti-*VEGFR-1* DNAzymes

To analyze the catalytic activity of the DNAzymes, *in vitro* cleavage testing was performed on an *in vitro* transcribed RNA of the soluble fraction of *VEGFR-1* gene. The results revealed that most of DNAzymes tested cleaved their substrate RNA efficiently (Figure 1). To screen the DNAzymes for their biological activity, we modified the DNAzymes with two phosphorothioate linkages at each end of the DNAzymes to increase the stability in cells. The modified DNAzymes were assayed in an *in vitro* angiogenesis Matrigel assay based on the differentiation of ECs and the formation of tubelike structures on an extracellular matrix (Matrigel). As shown in Table 1, seven out of 11 DNAzymes had an effect on the tube formation, among which DT18 showed the strongest effect (complete disruption of the tubelike structure). Thus, we selected DT18 as a lead molecule.

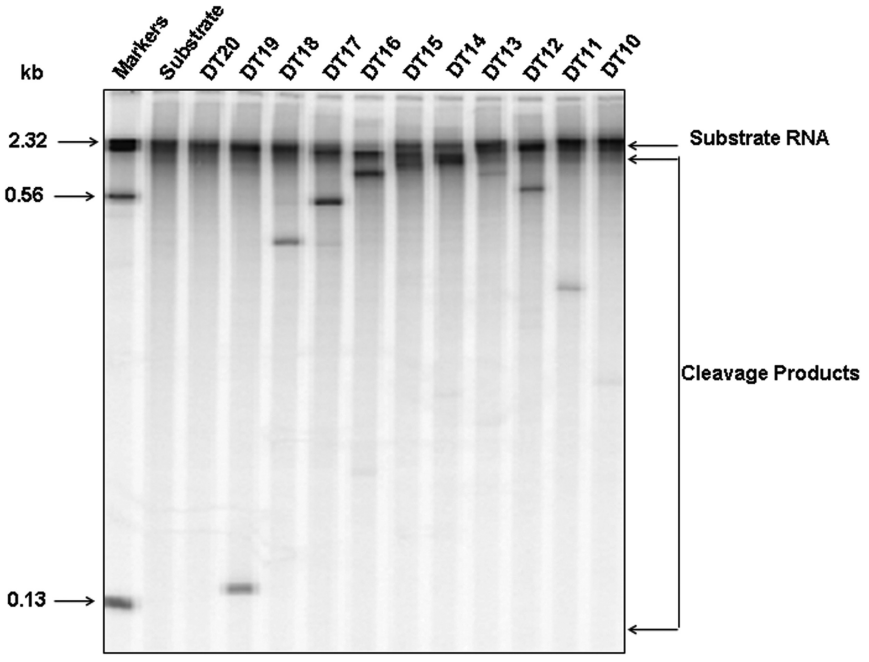

Figure 1. *In vitro* cleavage of *VEGFR-1* mRNA by DNAzymes. *In vitro* transcribed RNA with ^{32}P-labeling was incubated with individual DNAzyme in the cleavage buffer (50 mmol/L Tris-Cl, 10 mmol/L $MgCl_2$, pH 7.5). The samples were run on a 6% denaturing polyacrylamide gel and exposed on a PhosphorImager.

Molecular Characterization of DT18

To characterize DT18, a control molecule with an inverted catalytic core (INV-Ctrl, Figure 2A) was designed to exclude a potential antisense effect. We first examined DT18 kinetic features of the catalytic activity. The kinetics analysis was performed on a ^{32}P-labeled synthetic RNA substrate under a single turnover condition where 10-fold excess of DT18 was used in the presence of 10 mmol/L $MgCl_2$ (pH 7.2). The first order rate constant (k_{obs}) was measured as 0.103 min (Figure 2A), suggesting the favorable kinetic property of DT18.

We then determined the transfection efficiency by using TMP as a carrier. As shown in Figure 2B, a charge ratio of 3 gave an 80% transfection efficiency and over 90% cell viability. To examine whether the DNAzyme specifically downregulated the expression of the VEGFR-1 protein, Western blots were performed using the transfected HUVECs. Compared with controls, DT18 significantly inhibited target gene expression (Figure 2C), which was consistent with its cellular activity in blocking the tube formation (Figure 2D). These data suggest that DT18 can specifically and efficiently cleave its target both *in vitro* and in cells.

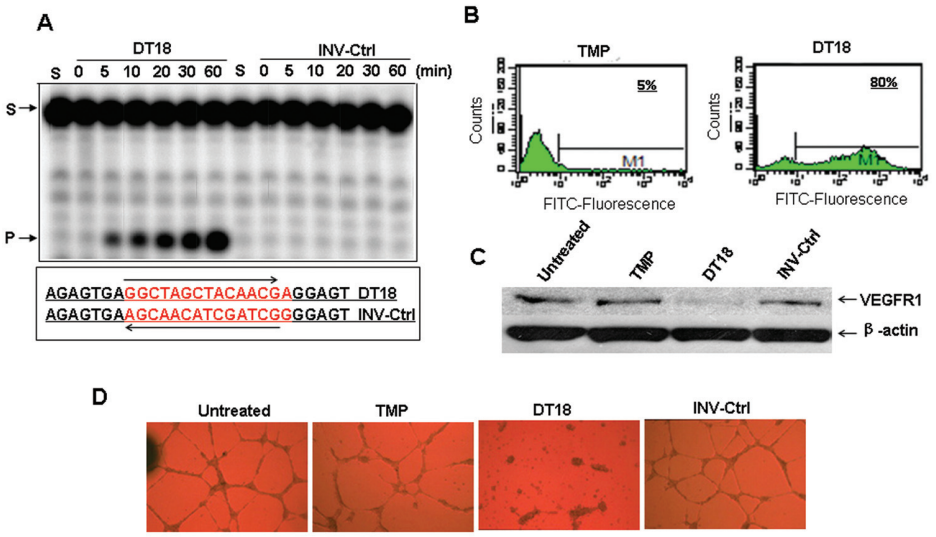

Figure 2. Molecular and cellular assays for DT18. (A) DT18 was assayed for its kinetic activity under a single turnover condition. Control was made with the same arms and an inverted catalytic core. The first order rate constant (k_{obs}) was used to determine the cleavage efficiency. (B) Transfection efficiency of DT18 was measured using FITC-labeled DT18 in HUVECs by FACS. TMP was used as a transfection reagent. (C) Effect of DT18 on VEGFR-1 expression in HUVECs was examined by Western blot. (D) Matrigel tube formation assay was performed to assess the antiangiogenic activity of DT18.

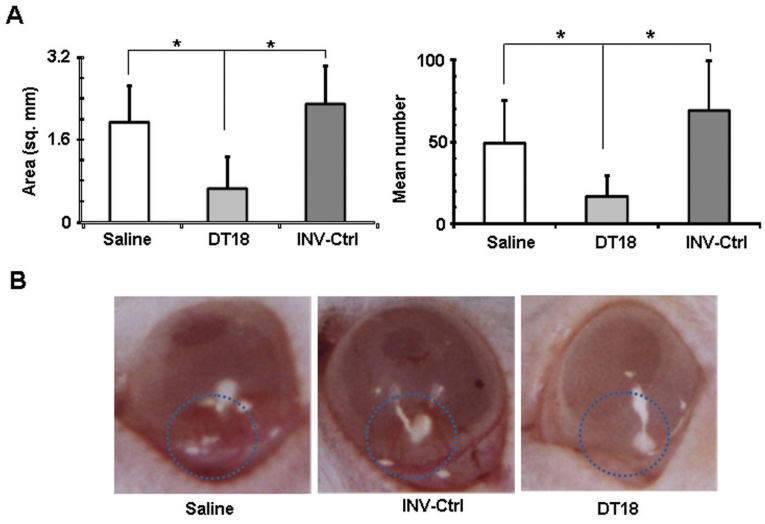

Figure 3. Effect of DT18 on neovascularization in rat cornea. The corneas of 7-wk-old male Sprague Dawley rats were implanted with a 30 μmol/L VEGF-soaked nitrocellulose filter disk. A total of 100 μg DT18, or its control oligonucleotides, was administered to the conjunctiva adjacent to the implant site on the day of disk implantation. The corneas were removed to quantitate the area covered by vascularization (A, left) and the number of vessels growing within the cornea (A, right). The representative photographs of the rat corneas from each group were shown in (B). Values are the means ± SE of three replicates. *$P < 0.05$ compared with the control.

Antiangiogenesis Activity of DT18

We examined the antiangiogenic activity of DT18 in a rat corneal pocket assay. Figure 3 represents the measurements of area of vascularization and vessel number. Clearly, there was a strong inhibition of angiogenesis by the *VEGFR-1* DNAzyme DT18, but not its control oligonucleotide INV-Ctrl in two independent experiments, each with at least five rats per group. When measuring area of vascularization, the inhibitions due to DT18 were 72.0% compared with the saline group. When counting the number of vessels growing from the limbus, the inhibitions due to DT18 were 61.0% compared with the saline group. Thus, both these methods of measurement indicated an antiangiogenic nature of the DT18. No difference in animal weights was noted between groups in two independent experiments. As a measure to check whether the surgical procedure itself induced neovascularization in the cornea, disks not soaked with VEGF were implanted, and these disks failed to induce a vascular response when implanted in the corneal pocket.

Antitumor Activity of DT18 in Mouse Models

We established two mouse models for assessing DT18 antitumor activity. In a synergetic mouse melanoma model (B16), the testing results showed that there was significant inhibition of growth of B16 tumors by coinjected *VEGFR-1* DNAzyme DT18, whereas the effect was not observed in either INV-Ctrl or saline control mice ($P < 0.05$) (Figure 4A). No difference in animal weights was noted between groups in two independent experiments. To rule out a direct effect of the DNAzyme against the B16 cells, a cell culture experiment was devised. There was no significant effect of DT18 on B16 cell proliferation as measured by MTT assays (Figure 4B). These data suggest that inhibition of B16 tumor growth was mediated by a direct effect on tumor angiogenesis, not on tumor cell proliferation.

To further examine the antitumor effect of DT18, a human xenograft mouse

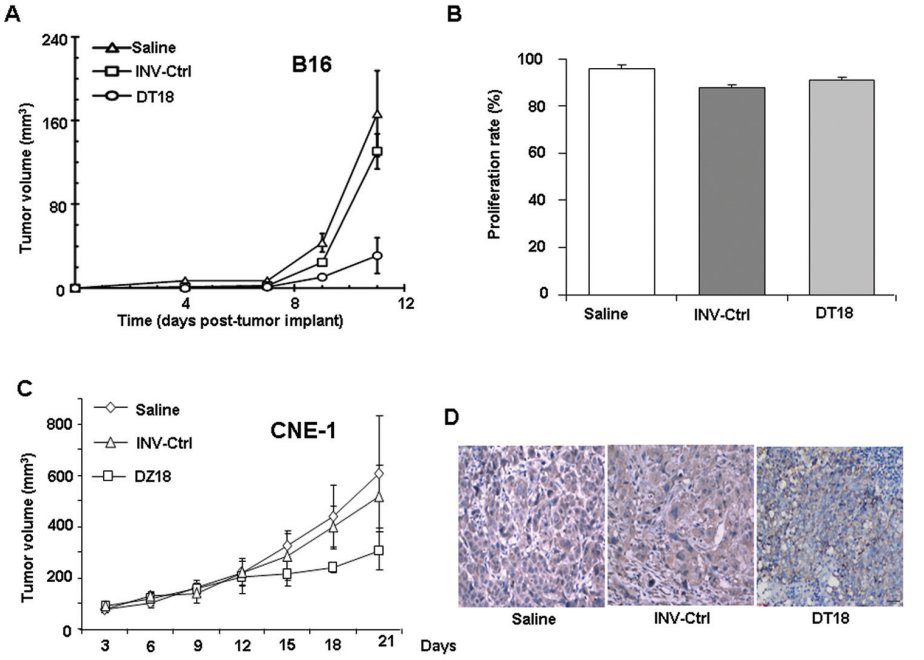

Figure 4. Antitumor effect of DT18. (A) DT18 was coinjected with B16 tumor cells into mice, and tumor volume was measured (n = 8). (B) Effect of Dt18 on B16 cell proliferation was measured by using MTT assay. (C) Human nasopharyngeal carcinoma was grown in nude mice, and DT18 mixed with Fugene6 was injected intratumorally when the tumor reached about 60–100 mm^3. Injections were made twice a week and tumor volumes were measured on alternate days (n = 5). (D) Immunohistochemical staining of the tumor tissues with the VEGFR-1-specific antibody in DT18-, INV-Ctrl– or saline-treated mice.

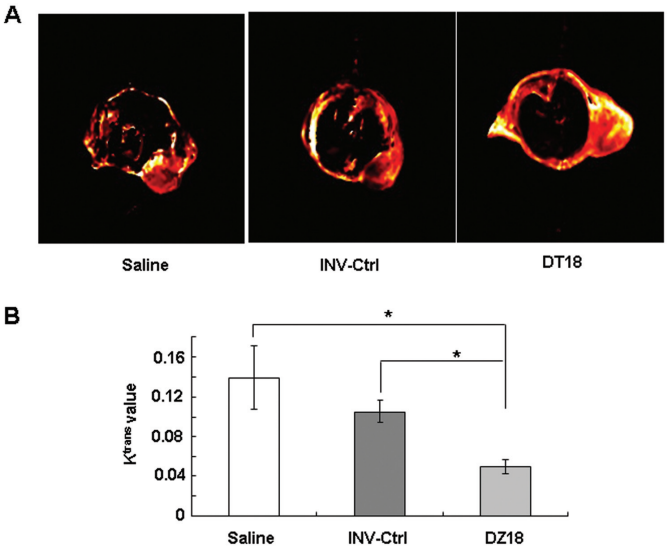

Figure 5. Effect of DT18 on tumor vasculature assayed by DCE-MRI. MRI was performed 3 d after the DT18 treatment on superconducting magnetic resonance imaging scanners (GE Signa HDx 3.0T) with 2.0 inches coil (FT-AN). Gd-DTPA, a blood-pool contrast agent, was injected via the tail-vein catheter. The representative images were presented (A). K^{trans} was generated from raw data of DCE-MRI by using NordicICE software (version 2.3.6) (B). Values are the means ± SE of three replicates. *$P < 0.05$ compared with the control.

model of NPC was established and used for assessing antitumor efficacy of DT18. As shown in Figure 4C, a series of intratumoral injection of DT18 suppressed the tumor growth compared with INV-Ctrl– or saline-treated mice ($P < 0.05$). Immunohistochemical staining of the tumor tissues with the VEGFR-1-specific antibody showed a reduction of the VEGFR-1 expression in DT18-treated mice (Figure 4D).

Effect of DT18 on Tumor Vasculature

We next examined whether inhibition of VEGFR-1 expression by DT18 had any impact on tumor microvascular permeability using DCE-MRI (Figure 5A). The parameter of K^{trans} (volume constant for transfer of contrast agent) derived from DCE-MRI has been widely used for evaluation of antitumor drugs (29). We compared the K^{trans} values of the DT18-, INV-Ctrl– or saline-treated mice and found significant differences between DT18 and INV-Ctrl ($P = 0.028$) or saline ($P = 0.026$) groups (Figure 5B), which indicated that DT18 inhibition of the VEGFR-1 expression in mice caused change of tumor vasculature and vessel permeability.

Safety and Pharmacokinetics of DT18

Toxicology studies are essential for the evaluation of candidate drugs. After a single intravenous administration of DT18 (20 mg/kg), DT18 safety and tolerability was demonstrated by several criteria. DT18 did not adversely affect body weight (Figure 6A), food intake and tissue index (Table 2) when administered intravenously in mice. No significant clinical hematology, clinical biochemistry, necropsy or organ histological treatment–related changes were observed (Figure 6B, Tables 3 and 4). Moreover, DT18 did not affect the proportion of T cells (Table 5), indicating that the antitumor effect of DT18 was not caused by activating the immune system. Pharmacokinetics of DT18 after intravenous administration in mice showed rapid elimination from the plasma compartment (Table 6). The parameters generated from the pharmacokinetic study showed a

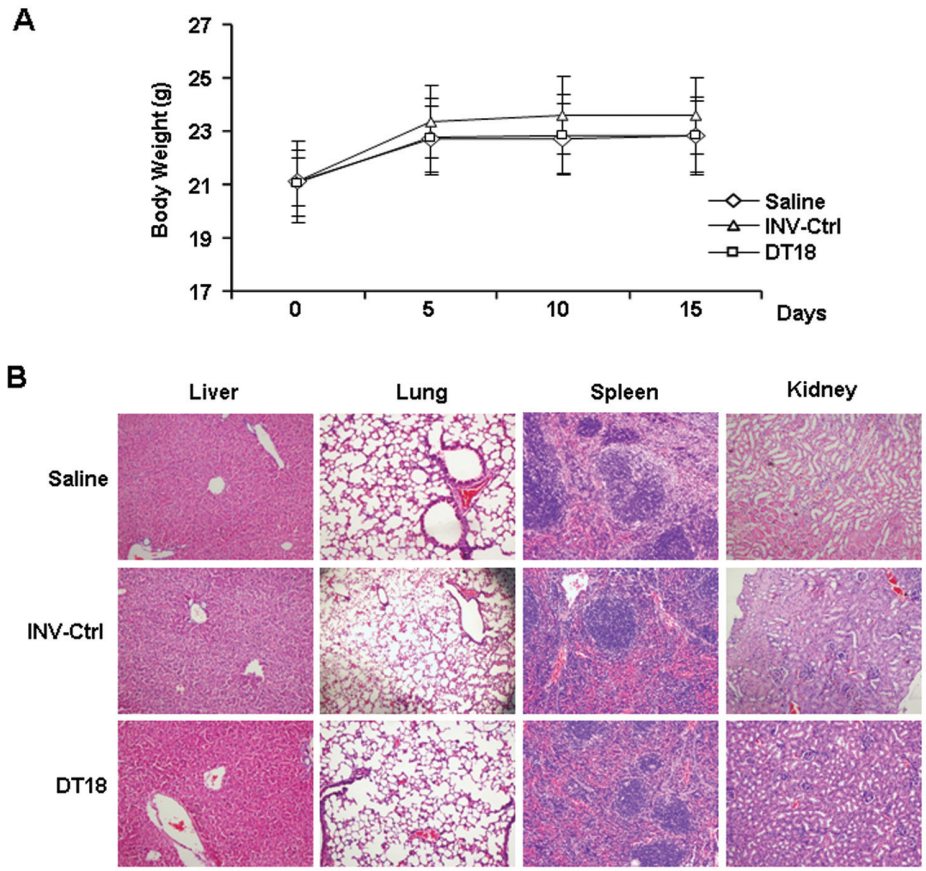

Figure 6. *In vivo* assessment of DT18 toxicity. (A) Effect of intravenously injected DT18 on body weight (n = 6). (B) Representative hematoxylin and eosin–stained sections of liver, lung, spleen and kidney from mice treated with DT18, INV-Ctrl or saline.

similar profile to that observed in mice previously (30). These data suggest that DT18 may be safe and well tolerated for potential clinical application.

DISCUSSION

Because of the pioneering work by Santoro and Joyce (15), DNAzymes have been explored for their therapeutic potentials. Clear advantages of the DNAzyme versus other RNA-targeting agents are its ease of chemical synthesis, broad target recognition properties and high catalytic turnover (17). Recently, a well-designed clinical trial demonstrated that a *c-jun*–targeted DNAzyme was efficacious and safe in patients with melanoma (23), which makes DNAzymes promising agents for clinical utility. Here, we demonstrate another example of the clinical potential of DNAzymes through careful choices of a therapeutic target mRNA that encodes VEGFR-1 and a disease setting in which the drug can be applied directly via injection into tumors in mouse models of skin and nasopharyngeal cancers.

During the past decades, antiangiogenic therapies have been pursued as a means of inhibiting tumor growth (12). One of the successful examples is Avastin, which is a humanized monoclonal antibody against VEGFA (31). Although Avastin is clearly beneficial to some cancer patients, the development of resistance to Avastin has been a major concern (32). The suggested mechanism of the Avastin resistance is that VEGF receptors have multiple ligands (such as VEGFs, fibroblast growth factors [FGFs] and placental growth factors [PIGFs]) and simply neutralizing VEGFA by Avastin may result in the resistance caused by alternative ligands (other than VEGFA) (14). Thus, targeting VEGF receptors has been suggested to be a strategy that could affect a broad range of signaling pathways involved in tumor angiogenesis. Here, we performed a comprehensive selection of the potential DNAzymes against *VEGFR-1* mRNA and obtained a lead molecule DT18. This molecule efficiently inhibited the VEGFR-1 expression, tube formation in matrigel and tumor growth in both syngeneic and xenograft models. This study demonstrates a successful alternative antiangiogenesis approach to cancer treatment

Table 2. Effect of DT18 on mouse well-being and tissue index.

Groups	Body weight gain (g)	Diet intake (g/d)	Liver index (mg/g)	Lung index (mg/g)	Spleen index (mg/g)	Renal index (mg/g)
Saline	1.71 ± 0.96	38.34 ± 5.09	48.33 ± 3.44	14.15 ± 1.45	4.02 ± 0.50	6.43 ± 0.44
INV-Ctrl	2.44 ± 0.58	42.39 ± 3.47	48.58 ± 3.20	13.67 ± 2.11	3.93 ± 0.72	6.44 ± 0.72
DT18	1.77 ± 0.91	39.01 ± 5.32	47.53 ± 2.98	13.60 ± 1.78	4.24 ± 1.05	6.37 ± 1.01
F value	2.362	2.976	0.292	0.276	0.404	0.025
P value	0.113	0.063	0.749	0.761	0.672	0.976

Data are expressed as mean ± SE and analyzed by one-way ANOVA followed by the Dunnett test (n = 5).

Table 3. Effect of DT18 on biochemical parameters in mice.

	Alanine aminotransferase	Aspartate aminotransferase	Blood urea nitrogen	Serum creatinine
Saline	52.37 ± 23.96	120.17 ± 17.35	6.8 ± 1.0	26.96 ± 15.64
INV-Ctrl	30.73 ± 3.31	116.55 ± 30.94	6.64 ± 0.99	50.78 ± 43.17
DT18	54.22 ± 22.2	138.08 ± 26.06	7.08 ± 0.94	52.77 ± 43.8
F value	1.443	0.863	0.232	0.765
P value	0.292	0.454	0.796	0.478

Data were analyzed by one-way ANOVA followed by the Dunnett test. The DT18 group was compared with the saline group and INV-Ctrl group (n = 5).

Table 4. Hematological parameters.

	Erythrocytes (10^{12} g/L)	Leucocytes (10^9 g/L)	Hemoglobin (g/L)	Platelets (10^9 g/L)	Neutrophil (10^9 g/L)	Lymphocytes (10^9 g/L)
Saline	8.89 ± 0.56	2.85 ± 0.74	154.25 ± 4.65	1024.5 ± 84.5	0.25 ± 0.23	2.55 ± 0.79
INV-Ctrl	8.94 ± 0.23	2.50 ± 0.47	153.8 ± 2.95	944.8 ± 84.2	0.38 ± 0.13	1.92 ± 0.65
DT18	8.90 ± 0.14	2.60 ± 1.26	151.2 ± 2.17	997.8 ± 99.3	0.32 ± 0.33	2.22 ± 0.92
F value	0.032	0.175	1.192	0.931	0.31	0.695
P value	0.969	0.842	0.340	0.423	0.739	0.520

Data were analyzed by one-way ANOVA followed by the Dunnett test. The DT18 group was compared with the saline group and INV-Ctrl group (n = 5).

by using a sequence-specific DNAzyme targeting *VEGFR-1*.

Because the upregulated expression of VEGF receptors is correlated with tumor angiogenesis, progression and metastasis (12), targeting the receptors on ECs has been recognized as a rational strategy for cancer treatment. In the present study, DT18 exhibited a strong suppression of tumor growth. To confirm that this activity is related to the impact of DT18 on the tumor vasculatures, transfection of DT18 into ECs showed a significant disruption of the EC differentiation, as evidenced by the distorted tube formation, while it had no effect on the tumor (B16) cell proliferation. Furthermore, by measuring the *in vivo* tumor vessel permeability with DCE-MRI, DT18 was shown to efficiently reduce K^{trans}, which indicated that suppression of VEGFR-1 on EC cells could change the tumor vasculature, leading to inhibition of tumor growth.

For antiangiogenic approaches, one of the concerns is the potential impact on normal vasculatures. VEGFR-1 evolved to have higher affinity to bind various ligands and lost its potency in kinase activity, creating a unique mechanism to control VEGFR-2 function by forming heterodimers with VEGFR-2, while VEGFR-2 plays a broader role in angiogenesis (33). Mechanistically, targeting either *VEGFR-1* or *VEGFR-2* should have similar antitumoral effects, as shown in the present study and the study by Zhang *et al.* (34). However, inhibition of VEGFR-1 would be expected to have less potential to generate toxic effect. Here, we show that DT18, in its modified form, is safe in a series of toxicology studies. No toxicity was evident in a mouse toxicology study, including clinical chemistry, hematological and histological parameters. No alteration in the percentage of CD4 and CD8 lymphocytes was reported at the intravenous dose of 20 mg/kg, indicating that DT18 had no immunotoxicity.

Table 5. Proportion of T-lymphocyte subsets of mice treated with DT18.

	$CD3^+$ (%)	$CD4^+$ (%)	$CD8^+$ (%)
Saline	6.50 ± 1.35	8.02 ± 0.98	2.78 ± 0.56
INV-Ctrl	6.91 ± 1.46	8.95 ± 1.15	3.03 ± 0.42
DT18	7.19 ± 1.68	8.95 ± 1.09	3.19 ± 0.27
F value	0.620	3.120	1.718
P value	0.733	0.210	0.424

Data were analyzed by one-way ANOVA followed by the Dunnett test. The DT18 group was compared with the saline group and INV-Ctrl group (n = 5).

CONCLUSION

These studies demonstrate that targeting *VEGFR-1* is safe, and DNAzymes are potentially suitable as drug candidates for further clinical evaluation.

ACKNOWLEDGMENTS

We would like to thank Crispin Dass for technical assistance in animal experimentation. This work was partly supported by the National Natural Science Foundation of China (81172188, 91129709, 81072220 and 81000596) and the PhD Graduate Supervision Fund of Ministry of Education, China (20110162110010).

DISCLOSURE

The authors declare that they have no competing interests as defined by *Molecular Medicine*, or other interests that might be perceived to influence the results and discussion reported in this paper.

Table 6. Determination of DT18 pharmacokinetics in mice.

	DT18 PK parameters				
Dose (mg/kg)	$T_{1/2}\alpha$ (h)	$T_{1/2}\beta$ (h)	C_{max} (mg/mL)	AUC (mg/mL h)	V_d (mL/kg)
10	0.1	46.7	84.4	97	890

The two-compartmental model of intravenous bolus injection best fit the plasma concentration-time curve. $T_{1/2}\alpha$, distribution half-life; $T_{1/2}\beta$, elimination half-life; C_{max}, maximum concentration; AUC, area under the curve; V_d, volume of distribution.

REFERENCES

1. Chung AS, Ferrara N. (2011) Developmental and pathological angiogenesis. *Annual Review of Cell and Developmental Biology.* 27:563–84.
2. Adams RH, Alitalo K. (2007) Molecular regulation of angiogenesis and lymphangiogenesis. *Nat. Rev. Mol. Cell Biol.* 8:464–78.
3. Augustin HG, Koh GY, Thurston G, Alitalo K. (2009) Control of vascular morphogenesis and homeostasis through the angiopoietin-Tie system. *Nat. Rev. Mol. Cell Biol.* 10:165–77.
4. Potente M, Gerhardt H, Carmeliet P. (2011) Basic and therapeutic aspects of angiogenesis. *Cell.* 146:873–87.
5. Carmeliet P, Jain RK. (2011) Molecular mechanisms and clinical applications of angiogenesis. *Nature.* 473:298–307.
6. Friesel RE, Maciag T. (1995) Molecular mechanisms of angiogenesis: fibroblast growth factor signal transduction. *FASEB J.* 9:919–25.
7. Gerber HP, Condorelli F, Park J, Ferrara N. (1997) Differential transcriptional regulation of the two vascular endothelial growth factor receptor genes: Flt-1, but not Flk-1/KDR, is up-regulated by hypoxia. *J. Biol. Chem.* 272:23659–67.
8. Carmeliet P, *et al.* (2001) Synergism between vascular endothelial growth factor and placental growth factor contributes to angiogenesis and plasma extravasation in pathological conditions. *Nat. Med.* 7:575–83.
9. Cherrington JM, Strawn LM, Shawver LK. (2000) New paradigms for the treatment of cancer: the role of anti-angiogenesis agents. *Adv. Cancer Res.* 79:1–38.
10. Ferrara N. (1997) The Role of Vascular Endothelial Growth Factor in the Regulation of Blood Vessel Growth. In: *Tumour Angiogenesis*. Bicknell R, Lewis CE, Ferrara N (eds.) Oxford University Press, New York, pp. 185–98.
11. Ellis LM, Takahashi Y, Liu W, Shaheen RM. (2000) Vascular endothelial growth factor in human colon cancer: biology and therapeutic implications. *Oncologist.* 5 Suppl 1:11–15.
12. Ivy SP, Wick JY, Kaufman BM. (2009) An overview of small-molecule inhibitors of VEGFR signaling. *Nat. Rev. Clin. Oncol.* 6:569–79.
13. Takahashi Y, Kitadai Y, Bucana CD, Cleary KR, Ellis LM. (1995) Expression of vascular endothelial growth factor and its receptor, KDR, correlates with vascularity, metastasis, and proliferation of human colon cancer. *Cancer Res.* 55:3964–8.
14. Chen CT, Hung MC. (2013) Beyond anti-VEGF: dual-targeting antiangiogenic and antiproliferative therapy. *Am. J. Transl. Res.* 5:393–403.
15. Santoro SW, Joyce GF. (1997) A general purpose RNA-cleaving DNA enzyme. *Proc. Natl. Acad. Sci. U. S. A.* 94:4262–6.
16. Sun LQ, Cairns MJ, Saravolac EG, Baker A, Gerlach WL. (2000) Catalytic nucleic acids: from lab to applications. *Pharmacol. Rev.* 52:325–47.
17. Rossi JJ. (2012) Resurrecting DNAzymes as sequence-specific therapeutics. *Sci. Transl. Med.* 4:139fs120.
18. Bhindi R, *et al.* (2007) Brothers in arms: DNA enzymes, short interfering RNA, and the emerging wave of small-molecule nucleic acid-based gene-silencing strategies. *Am. J. Pathol.* 171:1079–88.
19. Cairns MJ, Hopkins TM, Witherington C, Wang L, Sun LQ. (1999) Target site selection for an RNA-cleaving catalytic DNA. *Nat. Biotechnol.* 17:480–6.
20. Santiago FS, *et al.* (1999) New DNA enzyme targeting Egr-1 mRNA inhibits vascular smooth muscle proliferation and regrowth after injury. *Nat. Med.* 5:1264–9.
21. Yang L, Lu Z, Ma X, Cao Y, Sun LQ. (2010) A therapeutic approach to nasopharyngeal carcinomas by DNAzymes targeting EBV LMP-1 gene. *Molecules.* 15:6127–39.
22. Cai H, *et al.* (2012) DNAzyme targeting c-jun suppresses skin cancer growth. *Sci. Transl. Med.* 4:139ra182.
23. Cho EA, *et al.* (2013) Safety and tolerability of an intratumorally injected DNAzyme, Dz13, in patients with nodular basal-cell carcinoma: a phase 1 first-in-human trial (DISCOVER). *Lancet.* 381:1835–43.
24. Glaser R, *et al.* (1989) Two epithelial tumor cell lines (HNE-1 and HONE-1) latently infected with Epstein-Barr virus that were derived from nasopharyngeal carcinomas. *Proc. Natl. Acad. Sci. U. S. A.* 86:9524–8.
25. Santoro SW, Joyce GF. (1998) Mechanism and utility of an RNA-cleaving DNA enzyme. *Biochemistry.* 37:13330–42.
26. Cairns MJ, King A, Sun LQ. (2003) Optimisation of the 10–23 DNAzyme-substrate pairing interactions enhanced RNA cleavage activity at purine-cytosine target sites. *Nucleic Acids Res.* 31:2883–9.
27. Parry TJ, *et al.* (1999) Bioactivity of anti-angiogenic ribozymes targeting Flt-1 and KDR mRNA. *Nucleic Acids Res.* 27:2569–77.
28. Benimetskaya L, *et al.* (1998) Cationic porphyrins: novel delivery vehicles for antisense oligodeoxynucleotides. *Nucleic Acids Res.* 26:5310–5317.
29. Cheng HL. (2007) Dynamic contrast-enhanced MRI in oncology drug development. *Curr. Clin. Pharmacol.* 2:111–22.
30. Agrawal S, *et al.* (1991) Pharmacokinetics biodistribution and stability of oligonucleotide phosphorothioates in mice. *Proc. Natl. Acad. Sci. U. S. A.* 88:7595–9.
31. Bellou S, Pentheroudakis G, Murphy C, Fotsis T. (2013) Anti-angiogenesis in cancer therapy: Hercules and hydra. *Cancer Lett.* 2:219–28.
32. Ratner M. (2004) Genentech discloses safety concerns over Avastin. *Nat. Biotechnol.* 22:1198.
33. Rahimi N. (2006) VEGFR-1 and VEGFR-2: two non-identical twins with a unique physiognomy. *Front Biosci.* 11:818–29.
34. Zhang L, *et al.* (2002) Angiogenic inhibition mediated by a DNAzyme that targets vascular endothelial growth factor receptor 2. *Cancer Res.* 62:5463–9.